表3. NASH例の年齢・性，各組織変化，肥満・糖尿病

平均年齢＝54.8±12.2	(男性＝51±13) (女性＝56±12)	男女比＝28：50（女性64.1%）		
線維化の程度 (ALDの線維化に酷似)	F1 F3 *	23/78 (29%) 19/78 (24%)	F2 * F4 *	27/78 (35%) 9/78 (12%)
Nuclear Vacuolation		59/78 (76%) {(+)：32 (54%) (2+)：27 (46%)}		
Intracytoplasmic expression		40/78 (51%)		
Lipogranuloma		38/78 (49%)		
Mallory Body		26/78 (33%)		
Ceroid-lipofuscinosis		49/63 (78%) {(+)：37 (76%) (2+)：12 (24%)}		
Fe, granular siderosis		19/59 (32%)		
BMI (kg/m2)：1＝46 cases (59%), 2＝9 (12%), DM：about 60%				

*：3例のHCC合併例を含む　　(1990～2004. 3. 聖マ医大・関連病院経験78例)

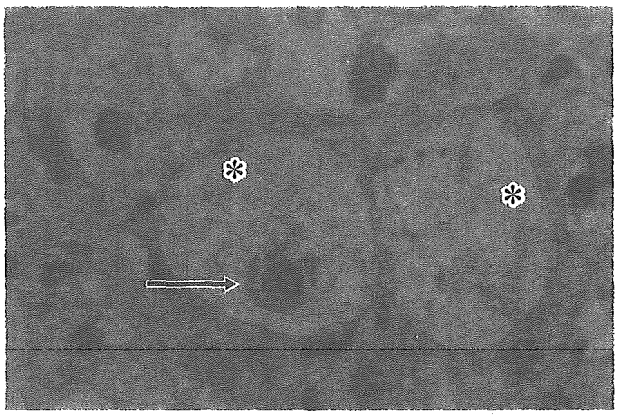

図4. 風船様膨化（＊）とMallory body（→）
Y.T., 34yrs. Female. DM, 肥満例, HE, ×40

脂肪滴に囲まれた部位に中等度までの肝細胞壊死がみられる[3]．また，間質-実質の境界である限界板は不分明化を呈するが，顕著な削り取り壊死（piecemeal necrosis）の形態ではなく細線維の伸長（図3-右）と細胆管の増生に依ることが多い[2,3]．

4）その他の実質域の変化

Matteoniら[4]やBruntら[1]は肝細胞の風船様膨化（図4）をNASHの組織変化の特徴として重視している．肝細胞の風船様膨化は一部の肝細胞で観察される例から，多数の肝細胞でみられる例までその程度は様々である．核空胞化は高頻度にみられ，ALDと比較してもNASHでは中等度以上かつびまん性で，目立つ例が多い[2,3]．胞体内凝集傾向は約半数に，約30%のNASH例にマロリー小体（Mallory body；MB）（図4）が出現する[3]．MBの性状はアルコール性脂肪性肝炎（alcoholic steatohepatitis；ASH）では太い棍棒状・鹿角状を呈するのに対し，NASHでは細く紐状であることが多い[3]．なお，ASHではMBの周囲に多数の好中球が遊走しているが，NASHでは少ない[3]．

5）門脈域の変化

門脈域への炎症性細胞浸潤は単核球主体で，その線維性拡大に比して弱い．筆者らはリンパ濾胞の形成を伴うNASHは経験したことがなく，リンパ濾胞が存在する例では別の要因を探るべきと考える[3]．なお，トランスアミナーゼが中等度以上に上昇した例では，実質内・門脈域に中等度までのCe-Lが観察される[2]．なお，ALDほどではないが，細胆管増生をみることが多い．

6）その他の変化

NASHでは胆汁うっ滞性変化は原則的には認めない．また，ベルリン・ブルー染色により3価鉄を観察すると，NASHの約1/3に鉄沈着がみられるが，過栄養性FLとは有意差はなく，オルセイン染色による観察でも銅の沈着はみられない．なお筆者らが鏡検した組織諸変化の分布と臨床像を参照されたし（表3）[3]．

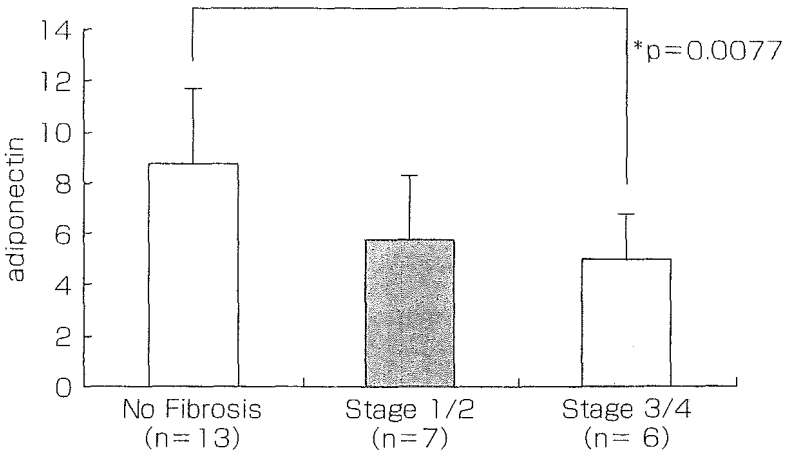

図5. NAFLDの線維化の進展と血清アディポネクチン値

2. NASHの臨床病理—その進展と予後

FLからNASH進展にはtwo hits theory[5]の考えが支持されており，第一段階としてFL，第二段階として酸化ストレス，脂質過酸化，インスリン抵抗性，種々の脂肪由来のサイトカイン，エンドトキシン，などにより肝障害が増悪してNASHに至ると考えられている．

横浜市立大学医学部消化器内科で経験したFLとNASHの肝組織の57,000余の網羅的遺伝子解析[6]では，NASHでFLに比し2倍以上上昇している遺伝子は，炎症（Gene；IGLJ3，TNFRSF6，CRP，LBP），線維化（Gene；EFEMP1，Collagen type 1，alpha 1），酸化ストレス（Gene；GPX2）などであり，NASHで低下している遺伝子はミトコンドリア機能異常(Magmas，MRPS 18B，NDUFB8，CYC1，ATP5D），金属代謝異常（MT1K，FDX1），アルコール代謝異常（ALDH1B1），アポトーシス関連(HNLF)であった[6]．これらの成績はFLからNASHに至るtwo hitをよく反映しているものと思われる[6]．またNAFLDでの線維化の程度と血中アディポネクチン値との関連では，アディポネクチンは線維化の進展と共に減少していた（図5）[7]．従ってNAFLDにおいて生成されるアディポネクチンなどの生理活性物質の動態解析はNASHの病態生理を究明する手掛かりとなると思われる．

Matteoniら[4]はNAFLDを4つの群に分けNAFLDの予後を検討した．4つの群とは，class 1；脂肪肝のみの群，class 2；脂肪肝と小葉内に炎症所見が加わった群（非特異的な実質炎が加わった脂肪肝），class 3；脂肪化と肝細胞の風船様膨化をみる群，class 4；さらにマロリー小体の出現や線維化が加わった群，に分けた．Matteoniらはclass 3，4をあわせたものがNASHであると提言している[4]．これは10年間の観察で，class 1，2の症例は3.4%しか肝硬変に進展しなかったことに対し，class 3，4の症例では24.7%が肝硬変に進展し，10年生存率も15%と59%と著明な差が認められたと報告している[4]．わが国のNASHに関する予後についての報告は未だない．

おわりに

わが国におけるNASHは最近注目を浴びたばかりで，臨床的に重要な慢性肝疾患として俎上に上ったばかりである．今はワンポイントにおける肝生検での診断例ばかりの集積であり，さらにNASHを診断する上で組織学的な診断基準での混乱もみられる．FLからNASHへのルートも不明な点が多く，未だ初期NASHから硬変期へと経時的に観察した例はほとんどない．

わが国では「健康21世紀」が今叫ばれている

が，現状はmetabolic syndromeの範疇に入るFLとNASHが蔓延しており，その対策は新たなそして重要な課題である．

文　献

1) Brunt EM : Nonalcoholic steatohepattis. Semin Liver Dis 24 : 3-24, 2004.
2) 前山史朗：脂肪肝・非アルコール性脂肪性肝炎(NASH)—その臨床病理と病因—．現代医療　33 : 2385-2394, 2001.
3) 前山史朗：非アルコール性脂肪性肝炎（NASH）の生検診断—NASHとALDとの比較—．病理と臨床　23 : 256-263, 2005.
4) Matteoni CA, et al:Nonalcoholic fatty liver disease:a spectrum of clinical and pathological severity. Gastroenterology 116 : 1413-1419, 1999.
5) Day CP, James OF : Steatohepatitis : a tale of two "hits" ? Gastroenterology 114 : 842-845, 1998.
6) 米田正人，他：糖尿病と肝臓死．Medical Practice 22 : 1731-1736, 2005.
7) Yoneda M, et al : Hypoadiponectinemia plays a crucial role in the development of nonalcoholic fatty liver disease (NAFLD) in patients with type 2 diabetes mellitus independently of insulin resistance and visceral adipose tissue. Alcohol Clin Exp Res 30, submitted, 2006.

2型糖尿病合併 non-alcoholic fatty liver disease（NAFLD）患者の肝臓内脂肪沈着，線維化形成に関与する内臓脂肪，adipocytokines の解析

横浜市立大学大学院医学研究科分子消化管内科学
米田　正人　　藤田　浩司　　中島　淳
横浜市立大学大学院医学研究科分子糖尿病・内分泌内科学
岩崎　知之　　寺内　康夫
北柏リハビリ総合病院
前山　史朗

1．はじめに

非アルコール性脂肪性肝炎（non-alcoholic steatohepatitis: NASH）の発症には2nd hit theoryが考えられている[1]．1st hitとして肝臓への脂肪沈着をきたし，2nd hitとしてさまざまなストレスや肝障害因子が加わり，炎症の持続や線維化の進展により肝硬変から肝癌，肝不全をきたしうる病態である．近年，2型糖尿病の合併[2),3)]，インスリン抵抗性，肥満など生活習慣病と脂肪肝，NASHとの関連はますます重要視されている．

脂肪細胞は単なるエネルギーの貯蔵庫ではなく，さまざまなサイトカイン（アディポサイトカイン）を分泌する生体内最大の内分泌臓器として認知されている．中でもアディポネクチンは抗動脈硬化作用[4]，抗高血圧作用[5]，抗糖尿病作用[6]を持っており，肥満時にその血中濃度が低下することや[7]，生活習慣病や心筋梗塞の発症[8]とも関わっていることが報告されている．

今回，我々は日本人の2型糖尿病患者における脂肪肝形成にかかわるアディポネクチンの関与を検討するために，血中のアディポネクチン濃度の測定を行った．その結果を，アディポサイトカインの一種であるレプチンや肝機能，インスリン抵抗性，またCTで測定した脂肪肝の程度，腹部内臓脂肪量との比較検討を行った．また単純性脂肪肝，NASH症例の肝生検所見を用い，アディポネクチンの肝線維化の進展にかかわる影響に関しても検証した．

2．対象と方法

対象は2004年1月から12月までに，当院の糖尿病科に通院している2型糖尿病患者のうちインスリン治療やチアゾリジン誘導体による治療を受けている患者を除外し，NAFLD，NASH以外の肝疾患を持ってない258人を対象とした．また当院に入院し肝生検を施行した2型糖尿病患者のうち（1）アルコール摂取量が20g/日以下　（2）Matteoniの分類[9]でclass 1を単純性脂肪肝，

Nonalcoholic fatty liver disease in Japanese patients with type 2 diabetes mellitus: relations to visceral adipose tissue and adipocytokines.

Masato Yoneda*1, Koji Fujita*1, Atsushi Nakajima*1, Tomoyuki Iwasaki*2, Yasuo Terauchi*2, Shiro Maeyama*3.
*1 Department of Gastroenterology, Yokohama City University School of Medicine. *2 Department of Endocrinology and Metaboliism, Yokohama City University School of Medicine. *3 Kitakashiwa Rehabilitation Hospital.

class3，4をNASHと分類 (3) 他のウイルス性，代謝性，自己免疫性肝疾患などが否定できたものを用い血清アディポネクチン濃度と線維化の検討に用いた．肝生検の線維化の分類はBruntの分類[10]に従い，F0（線維化なし），F1-2（線維化軽度），F3-4（線維化高度）と群別を行った．血清アディポネクチン濃度，レプチン濃度はELISA法で測定を行った．インスリン抵抗性の指標としてhomeostasis model assessment insulin resistance（HOMA-IR）の測定を用いた．肝臓の脂肪含有量の測定は腹部CTでの肝臓と脾臓のCT値比[11]（Liver to spleen ratio: L/S比）を用い定量化を行った．また内臓脂肪，皮下脂肪量の定量として臍レベルでのCT断面像より内臓脂肪計測ソフト（Fat Scan R:N2 システム株式会社製）を用い測定を行った．

3．結　果

(1) 肝臓の脂肪含有量との関連

脂肪含有量の定量としてL/S比を測定し，血清ALT値，血清AST値，血清アディポネクチン濃度，血清レプチン濃度，腹部内臓脂肪量，腹部皮下脂肪量との関係を調べた．L/S比はAST値（$r=-0.459$，$p<0.0001$），ALT値（$r=-0.517$，$p<0.0001$），内臓脂肪量（$r=-0.376$，$p<0.0001$），皮下脂肪量（$r=-0.295$，$p<0.0001$）と有意な負の相関を認めた．またL/S比は血清アディポネクチン濃度（$r=0.300$，$p=0.0007$）と有意な正の相関を認めたが，血清レプチン濃度（$r=-0.203$，$p=0.0565$）とは相関を認めなかった（図1）．つまりL/S比が低値，すなわち肝臓の脂肪含有量が高度になるに従い血清AST値，血清ALT値，内臓脂肪量，皮下脂肪量は高値となり，血清アディポネクチン濃度は低値になる傾向を認めた．

(2) 血清アディポネクチン濃度との関連

2型糖尿病患者において血清アディポネクチン濃度はL/S比と正の相関を認めたが，血清AST値，血清ALT値，内臓脂肪量，皮下脂肪量，血清レプチン濃度との関係を調べた．血清アディポネクチン濃度は血清AST値（$r=-0.298$，$p=0.0006$），血清ALT値（$r=-0.298$，$p=0.0007$），内臓脂肪量（$r=-0.321$，$p=0.0002$）と有意な負の相関をみとめたが，皮下脂肪量（$r=-0.327$，$p=0.5456$），血清レプチン濃度（$r=-0.075$，$p=0.4763$）とは相関を認めなかった（図2）．

(3) 脂肪肝を形成する因子の多変量解析

脂肪肝成立に関する独立した因子を検証するために，HOMA-IR，内臓脂肪量，血清アディポネクチン濃度を用い年齢，性別を調節して多変量解析を行った．その結果，血清アディポネクチン濃

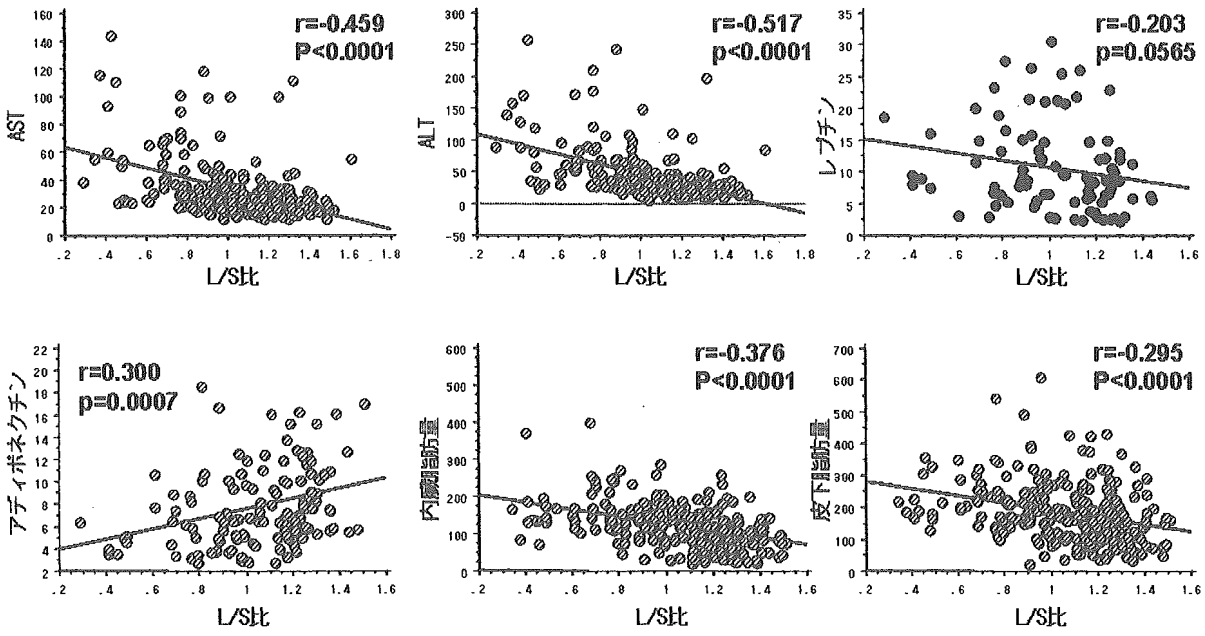

図1　肝臓内の脂肪蓄積量（L/S比）と各種データとの相関

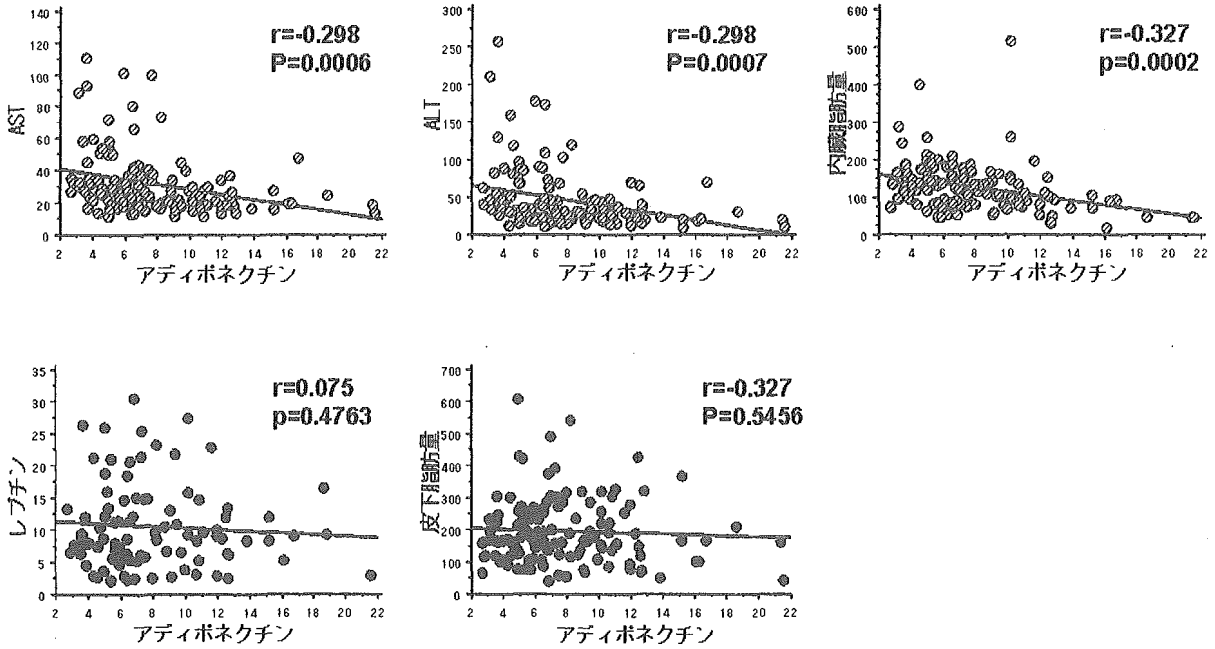

図2　血清アディポネクチン濃度と各種データとの相関

表1　各群における肝脂肪変性の程度

危険因子		標準回帰係数	標準誤差	*P*値
年齢	0.136	0.058	0.289	0.0225
性別	0.014	0.002	0.820	<0.0001
アディポネクチン	0.019	0.008	0.321	0.0223
内臓脂肪	1.605E-4	3.755E-4	0.428	0.6704
HOMA-IR	-0.001	0.006	-0.115	0.9091

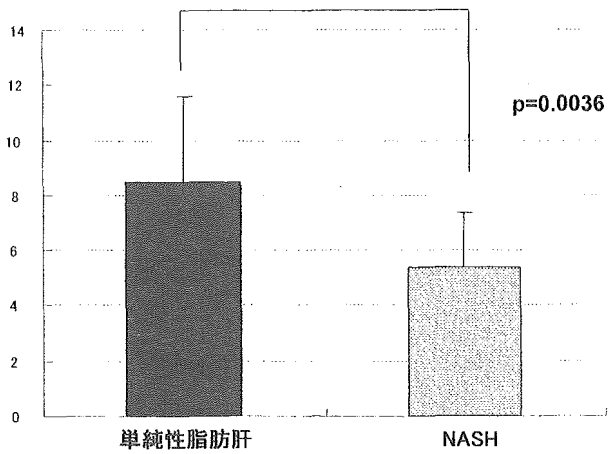

図3　単純性脂肪肝患者とNASH患者の血清アディポネクチン濃度

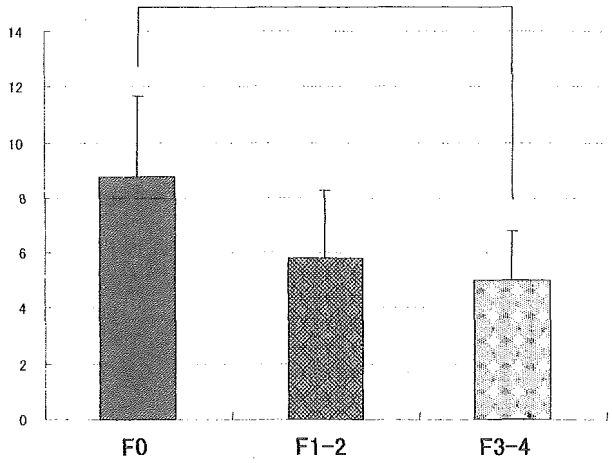

図4　血清アディポネクチン量と肝線維化

度は，脂肪肝の成立に関して，内臓脂肪量，インスリン抵抗性と独立した因子であった（p=0.0223）（表1）．

(4)　血清アディポネクチン濃度と肝臓内線維化との関連

血清アディポネクチン濃度は単純性脂肪肝患者と比べNASH患者で有意に低値であった（p=0.0036）（図3），また線維化別に群別した検討では血清アディポネクチン量は線維化の進行に伴い低下する傾向を示し，NASH　F3-4（線維化高度例）ではF0（線維化なし）群と比べ有意に低値であった（p=0.0077）（図4）．

4．考　察

近年，日本においても生活習慣の欧米化が進み，肥満，糖尿病，高脂血症など生活習慣病をもつ人口が増加している．その背景として脂肪細胞の増加，脂肪細胞より分泌されるさまざまなアディポサイトカインが関与していることが知られて

いる．今回私たちは，生活習慣病の一つとして考えられているNAFLD，NASHにおいて主にアディポネクチンがどのように関与しているかを，2型糖尿病患者において検討した．

まず肝臓の脂肪沈着量の定量を腹部単純CTでのL/S比で検討したところ，内臓脂肪，皮下脂肪の増加および，血清アディポネクチン濃度の低下が肝臓の脂肪化と強い相関を認めることが示唆された．しかし血清アディポネクチン濃度は内臓脂肪の蓄積に伴って低下することが報告されており，今回の測定においても血清アディポネクチン濃度の低下は腹部内臓脂肪量と強い相関を認めた．そのため血清アディポネクチン濃度の低下は，直接作用として肝臓の脂肪沈着に働くのか，腹部内臓脂肪量の増加が主に肝への脂肪沈着に関与し，血清アディポネクチン濃度は2次的に低下しているのかが疑問となった．そのため私たちは脂肪肝成立に関する独立した因子を検証するために，HOMA-IR，内臓脂肪量，血清アディポネクチン濃度を用い年齢，性別を調節して多変量解析を行ったところ，血清アディポネクチン濃度の低下はインスリン抵抗性，内臓脂肪量と独立した因子であることが証明された．

肝組織での線維化の検討においても単純性脂肪肝患者に比べ，NASH患者において血清アディポネクチン濃度は有意に低値であり，線維化の進展とともに低下する傾向を認めた．つまり血清アディポネクチン濃度の低下は内臓脂肪量，インスリン抵抗性と独立した因子として脂肪肝の成立（1st hit）をきたし，また脂肪肝から脂肪性肝炎への進展（2nd hit），線維化の進展にも関与する可能性が示唆された．今後のNAFLD，NASHの治療を考える上で，血清アディポネクチン濃度を増加させるようなダイエット療法の重要性が再認されると同時に，血清アディポネクチン濃度を上昇させるPPARγ（peroxisome proliferator-activated receptor γ）リガンドであるチアゾリジン誘導体もパイロットスタディーでのNASH患者への有効性が報告されており，今後の更なる検討が望まれる．

文　献

1）Day CP, James OF. Steatohepatitis: a tale of two "hits"? Gastroenterology 114: 842-845, 1998.
2）Clark JM, Diehl AM. Hepatic steatosis and type 2 diabetes mellitus. 2: 210-215, 2002.
3）Angulo P. Nonalcoholic fatty liver disease. N Engl J Med 346；1221-1231, 2002.
4）Funahashi T, Nakamura T, Shimomura I et al. Role of adipocytokines on the pathogenesis of atherosclerosis in visceral obesity. Intern Med. 38: 202-206, 1999.
5）Adamczak M, Wiecek A, Funahashi T, et al. Decreased plasma adiponectin concentration in patients with essential hypertension. Am J Hypertens. 16: 72-75, 2003.
6）Yamauchi T, Kamon J, Waki H, et al. The fat-derived hormone adiponectin reverses insulin resistance associated with both lipoatrophy and obesity. Nat Med. 7: 941-946, 2001.
7）Ryysy L, Hakkinen AM, Goto T, et al. Hepatic fat content and insulin action on free fatty acids and glucose metabolism rather than insulin absorption are associated with insulin requirements during insulin therapy in type 2 diabetic patients. Diabetes. 49: 49-58, 2000.
8）Hotta K, Funahashi T, Arita Y, et al. Plasma concentrations of a novel, adipose-specific protein, adiponectin, in type 2 diabetic patients. Arterioscler Thromb Vasc Biol. 20: 1595-1599, 2000.
9）Matteoni CA, Younossi ZM, Gramlich T, et al. Nonalcoholic fatty liver disease: a spectrum of clinical and pathological severity. Gastroenterology. 116: 1413-1419, 1999.
10）Brunt EM, Janney CG, Di Bisceglie AM, et al. Nonalcoholic steatohepatitis: a proposal for grading and staging the histological lesions. Am J Gastroenterol. 94: 2467-2474, 1999.
11）Wasnich R, Glober G, Hayashi T, et al. Simple computer quantitation of spleen-to-liver ratios in the diagnosis of hepatocellular disease. J Nucl Med. 20: 149-154, 1979.

臨床検査ガイド 2005~2006

これだけは必要な検査のすすめかた・データのよみかた

Medical Practice編集委員会 編

表5　AST/ALT による肝病態診断表

AST/ALT 比	疾患名
1. AST，ALT が基準範囲の5倍以上に上昇しうる病態	
>1	劇症肝炎，アルコール性肝炎，ルポイド肝炎
	心筋梗塞（重症），ショック，急性ウイルス肝炎（初期）
≦1	急性ウイルス肝炎，薬剤性肝炎，慢性活動性肝炎
2. 通常基準範囲の5倍以下の上昇にとどまる病態	
>2	肝癌，筋ジストロフィー
>1	肝硬変，原発性胆汁性肝硬変，うっ血性心不全，心筋梗塞（軽症）
	脂肪肝（アルコール），溶血
≦1	慢性非活動性肝炎，胆汁うっ滞，脂肪肝（過栄養性）
3. 基準範囲	
HB および HC ウイルスキャリア，突発性門脈圧亢進，塩化ビニール中毒	

予想外の値が得られた場合にはどうするか

1．検査過誤をチェックする

検査前の患者の状況，採血時の状況，検体の溶血，乳濁の有無，検体の運搬保存の状態，検査ミス．

2．再検する

3．関連データを検索する

肝疾患の疑い：γGTP，ALP，LDH アイソザイム，肝炎ウイルス検査（抗原，抗体検査）．

心疾患の疑い：ECG，CPK，LDH，CPK アイソザイム，LDH アイソザイム．

溶血性疾患の疑い：LDH，ハプトグロビン，血球検査，末梢血液像．

甲状腺機能異常の疑い：free T_4，TSH．

他の組織の病変：LDH，CPK．

ビタミン B_6 欠乏症の疑い：ピリドキサルリン酸を試薬に添加して測定する．

4．経過観察

異常値がみられた場合の検査の進め方と対応

① 既往症，現病歴，家族歴，理学所見などを再度確認する．体重，過去のデータ，飲酒量，使用中の薬，旅行した場所などを調べる．

② 関連データを調べる．

肝疾患：AST，ALT，LDH，LDH アイソザイム，LAP，γGTP，ビリルビン，総蛋白，A/G 比，血清蛋白電気泳動，総コレステロール，LCAT，IgM-HA 抗体，HBs 抗原，HCV 抗体，HCV-RNA など．

心疾患：心電図，CK，CK アイソザイム (CK-MB)，LDH，LDH アイソザイム，ミオグロビン，ミオシン軽鎖．

免疫グロブリン結合酵素：AST あるいは ALT のいずれかが長期間にわたって単独高値で他の関連データが基準範囲内の場合は，免疫グロブリン結合酵素の出現が考えられる．免疫グロブリン結合酵素は血中半減期が長いため，その酵素活性だけが高値となるので，治療に必要である．

長期間活性値が0付近の場合は阻害抗体の有無を調べる（高値血清と混合試験），阻害抗体がなければ，遺伝子異常を解析する場合もある．

文　献

1）大久保昭行：血清トランスアミナーゼ (GOT)，ALT (GPT))．臨床検査ガイド-2000．Medical Practice 編集委員会編，文光堂，p.117-121，1999

2）日本臨床化学会クオリティマネジメント委員会プロジェクト報告，福岡県における化学28項目の基準範囲と標準化．臨床病理 30：171-184，2001

3）Guder，W.G. et al.，清崎直孝ほか訳：検査の仕方一検体採取から測定まで．医歯薬出版，1998

4）和田　博ほか：アスパラギン酸アミノトランスフェラーゼ．臨床検査 32：1291-1300

1. 生化学検査／A. 酵素関係（アイソザイムを含む）

コリンエステラーゼ（ChE）

米田正人・中島　淳

デシジョンレベル（表1）

表1　デシジョンレベル

	方　針	高頻度にみられる疾患	否定できない疾患
異常低値	肝機能不全を疑う．全身状態の検索，各種画像検査を行う．特に腹水，食道静脈瘤に注意し必要があれば入院治療を	非代償性肝硬変	
高値	肝臓疾患と低栄養状態，感染症のチェックが必要．内服薬のチェック．原疾患の診断のため他の肝機能検査，血算，肝炎ウイルスマーカーの検索，各種画像検査を行う．必要があれば入院治療を	肝硬変/肝細胞癌，劇症肝炎，慢性肝炎の急性増悪，低栄養，敗血症などの急性重症感染症，各種の悪性腫瘍	有機リン中毒，各種の慢性消耗性疾患（膠原病，粘液水腫，下垂体・副腎不全，熱傷，天疱瘡，うっ血性心不全，潰瘍性大腸炎など），副交感神経刺激薬（ChE 阻害薬）の内服，遺伝性 ChE 異常症
基準域	アルコール性脂肪肝は否定できず	健康	アルコール性脂肪肝
高値	肝細胞での産生亢進，高栄養状態，蛋白合成や脂質代謝の亢進を反映する．原疾患の診断，治療を行う	非アルコール性脂肪肝，糖尿病，ネフローゼ症候群，甲状腺機能亢進症	肥満，本態性高 ChE 血症，肝細胞癌に伴う高 ChE 血症（腫瘍随伴症候群）

基準値（表2）

表2　ChE の基準値

測定法や施設により基準値が大幅に異なるので，測定法を確認のこと
pH 法・高橋法　0.6～1.2ΔpH
ブチルコリン基質—DTNB 比色法　3,000～7,000 IU/*l*
ベンゾイルコリンオキシダーゼ基質　782～1,494 U/*l*
p-HBC 基質　200～465 IU/*l*（女性　180～355 IU/*l*）
新生児　成人の80～90％
乳幼児～1歳児　成人の130％

血清 ChE はコリンエステルを水解して有機酸を遊出するため，その活性測定は緩衝液の pH 低下を測定することによって行う方法（pH 高橋法）が一般的である（基準値0.8～1.0 pH）．ChE は基質特異性が少ないため各種 acylcholine が基質として用いられ測定法により基準値は大幅に異なる．今日，基質として最も多く用いられているのは P. hydroxybenzoylcholine（*p*-HBC）である．その反応は *p*-HBC が ChE により加水分解され，コリンと *p*-ヒドロキシ安息香酸を生成し（第1反応），*p*-ヒドロキシ安息香酸は NADPH の存在下，4-ヒドロキシ安息香酸水酸化酵素によりプロトカテキュ酸に変換される（第2反応）．このときに酸化される NADPH の340nm における吸光度の減少よりコリンエステラーゼ活性を測定するものであり再現性に優れている（第2回臨床化学夏季セミナープログラム：79，1982）．

女性では男性よりも低値を示し，性ホルモンの影響で妊娠，月経時に低下する．新生児は成人の約80～90％，乳幼児は成人の130％の値をとり1歳から徐々に低下し成人の値に近づく．

測定上の注意

採血から分離まで室温，冷蔵で24時間以内では活性に変化はない．血清分離後は冷凍で1ヵ月まで安定．−80℃で数ヵ月．Ca^{2+} 除去で活性低下するため，血漿の場合はヘパリン採血を行う．

検査によって何がわかるか

ChEはコリンエステルをコリンと有機酸に加水分解する酵素であり生体内には2種類存在する．一つはアセチル-β-メチルチオコリンを特異的に水解するアセチルコリンエステラーゼで真性コリンエステラーゼtrue-cholinesteraseと呼ばれ，神経，筋肉，赤血球に存在し，コリン作動性神経でアセチルコリンを分解し神経系の刺激伝達に関与する．もう一つはアセチルコリンのほか種々のコリンエステル，エステルを加水分解する酵素で偽性コリンエステラーゼpseudo-cholinesteraseと呼ばれ，血清，肝，膵に多く存在し，肝で合成され血中に遊離する．臨床検査で測定するChEは血中の偽性ChEであり，血清中のChEの測定は肝での代謝機能を反映する．

どういうときに検査するか

肝機能の全体的な把握ができるため肝硬変や，慢性肝炎の重症度や治療の経過をみるのに用いられる．また脂肪肝，有機リン中毒の指標として用いられる．

異常となる疾患/異常となる薬物

1．血清ChE値が異常となる疾患

血清ChEの活性は肝臓の機能を反映するため肝機能検査としては本来低下が重要視されていた．急性肝炎では病状の推移に応じた動向を示し，進行性の肝疾患で肝硬変に至る例においては漸次低値となり，非代償性の肝硬変においては極度に持続低値を示す．慢性肝炎は基準値下限を示すことが多いが，慢性肝炎の急性増悪の際には低値を示す．そのため肝疾患における血清ChEの測定は急性肝炎の重症度判定，慢性肝疾患の大局的動向に重要であり，また胃潰瘍，赤痢など消化器疾患，悪性貧血，癌など栄養状態が低下するときは低値を示す．先天的に血清ChEの活性低下または欠損を認める場合があり，ジブカイン抵抗型（3,500人に1人），フルオランド抵抗型（15,000人に1人），サイレント抵抗型（100,000人に1人）と呼ばれる．

ChEが高値を示す疾患として非アルコール性の脂肪肝，ネフローゼ症候群が重要であり，また全体的な蛋白代謝の亢進を反映し肥満や甲状腺機能亢進症でも高値を示す．肝細胞癌にはときに高値を示す場合があり腫瘍随伴症候群と考えられる．

2．血清ChEが異常となる薬物

重症筋無力症用薬であるコリンエステラーゼ阻害薬（コリンエステラーゼを阻害することでアセチルコリンの分解を抑制し，シナプス間隙のアセチルコリン濃度を高める薬，ネオスチグミン，フィゾスチグミンほか）内服によるもの，また白血病治療薬のL-アスパラギナーゼの肝障害でも低下をきたす．また有機リン中毒ではChEのesteratic siteに作用し阻害を起こす．

検査の総合評価

血清コリンエステラーゼは肝臓で生成され血中を循環するため肝実質の蛋白合成機能を反映する．同じ肝臓で生成される血清アルブミン値と動向を一にしており，また近年の測定法の向上により肝機能の全体的な把握に適しており，大局的な肝機能の推移に繁用される．また全身の蛋白合成を反映するため肥満，糖尿病，脂肪肝など生活習慣病のコントロールの指標，甲状腺疾患のコントロールの指標にも有意義と考えられる．

予想外の値が得られた場合にはどうするか

血清コリンエステラーゼは肝臓が主要な生合成の場であり，かつ逸脱酵素ではないためにその値は肝機能の最も標準的な指標となる．そのため異常値を認めた際には肝疾患を念頭に肝[illegible]ウイルスの検索，腹部超音波，腹部CTなど画像検査を施行すべきである．また腎疾患，甲状腺疾患，生活習慣病（特に肥満，糖尿病）の精査も行わなくてはならない．

異常値がみられた場合の検査の進め方と対応

ChEの低値を認めた場合は肝疾患や[illegible]染症，悪性腫瘍を疑い原因疾患の診断を行う．肝炎ウイルスの検索，腹部超音波，腹部CT，胸部X線，各種腫瘍マーカーの検索，上部消化管検査を施行する．ChEが高値の[illegible]は脂肪肝の有無，甲状腺疾患（TSH，FT_4），腎疾患（尿蛋白），糖尿病（HbA1c，糖，血糖，75gOGTT），高脂血症の[illegible]

膵リパーゼ，エラスターゼ1，ホスホリパーゼA_2

越智浩二・白髭明典

デシジョンレベル（表1）

表1　デシジョンレベル

	方針	高頻度にみられる疾患	否定できない主要疾患
異常低値	膵機能の荒廃	慢性膵炎，膵切除後	膵癌，糖尿病（特にインスリン治療例）
基準値		健康	
軽度高値 基準域の3倍未満	膵疾患のみならず腎からの排泄低下も考慮する	急性膵炎，慢性膵炎，膵癌，腎不全	慢性膵炎，膵癌 腎不全，糖尿病，胆嚢，胆道疾患
著明高値 基準域の3倍以上	腹痛などがあれば，急性膵炎の加療 無症状であれば，膵癌の検索	急性膵炎，膵癌	

基準値（表2）

表2　基準値

リパーゼ	
比濁法	36～161IU/l
酵素法	8～25IU/l
合成基質法	46～130U/l
エラスターゼ1	
RIA法	70～430ng/dl
EIA法	2.9～19.2ng/ml
ホスホリパーゼA_2	
RIA法	130～400ng/dl

[illegible]法によって，基準値は大きく異なるので[illegible]要する．特にリパーゼは測定法や基質の[illegible]ずれの酵素も性差は認められず，高齢者[illegible]機能の低下などにより高値を示すことが[illegible]

[illegible]上の注意

[illegible]の酵素も日内変動や食事の影響は少な[illegible]の影響は認められない．

検査によって何がわかるか

いずれの酵素も膵臓の腺房細胞で合成され膵液中に分泌される消化酵素である．腺房細胞の障害があれば，血中に逸脱し，高値を示し，腺房細胞障害のマーカーである．

従来，膵逸脱酵素としてアミラーゼが頻繁に測定されてきたが，アミラーゼには膵型アミラーゼと唾液腺型アミラーゼの2種類があり，検査法が簡便な総アミラーゼの測定には膵特異性に欠けるという問題点があるが，これらの3酵素はいずれも総アミラーゼと比べ，膵特異性に優れている．

膵全摘後や慢性膵炎の進行例など膵が荒廃している場合には低値を示し，膵の残存機能を知ることができる．

エラスターゼ1は腫瘍マーカーに分類されることがあるが，基本的には膵逸脱酵素である．血中に長く残存するために，膵癌の随伴性膵炎の検出に有用である．

どういうときに検査するか

膵疾患が疑われる場合，膵癌のスクリーニング．

An *in vitro* model of hepatitis C virion production

Theo Heller*†, Satoru Saito*†, Jonathan Auerbach*, Tarice Williams*, Tzivia Rachel Moreen*, Allison Jazwinski*, Brian Cruz*, Neha Jeurkar*, Ronda Sapp*, Guangxiang Luo‡, and T. Jake Liang*§

*Liver Diseases Branch, National Institute of Diabetes and Digestive and Kidney Diseases, National Institutes of Health, Bethesda, MD 20892; and ‡University of Kentucky College of Medicine, Lexington, KY 40506

Communicated by Reed B. Wickner, National Institutes of Health, Bethesda, MD, December 23, 2004 (received for review November 29, 2004)

The hepatitis C virus (HCV) is a major cause of liver disease worldwide. The understanding of the viral life cycle has been hampered by the lack of a satisfactory cell culture system. The development of the HCV replicon system has been a major advance, but the system does not produce virions. In this study, we constructed an infectious HCV genotype 1b cDNA between two ribozymes that are designed to generate the exact 5′ and 3′ ends of HCV. A second construct with a mutation in the active site of the viral RNA-dependent RNA polymerase (RdRp) was generated as a control. The HCV-ribozyme expression construct was transfected into Huh7 cells. Both HCV structural and nonstructural proteins were detected by immunofluorescence and Western blot. RNase protection assays showed positive- and negative-strand HCV RNA. Sequence analysis of the 5′ and 3′ ends provided further evidence of viral replication. Sucrose density gradient centrifugation of the culture medium revealed colocalization of HCV RNA and structural proteins in a fraction with the density of 1.16 g/ml, the putative density of HCV virions. Electron microscopy showed viral particles of ≈50 nm in diameter. The level of HCV RNA in the culture medium was as high as 10 million copies per milliliter. The HCV-ribozyme construct with the inactivating mutation in the RdRp did not show evidence of viral replication, assembly, and release. This system supports the production and secretion of high-level HCV virions and extends the repertoire of tools available for the study of HCV biology.

assembly | cell culture | infection | ribozyme | viral replication

The hepatitis C virus (HCV) is an important cause of human illness worldwide (1). Although it has proven to be a difficult public health problem, it has been no easier to study in the laboratory. A major impediment has been the lack of robust model systems to study the complete viral life cycle. HCV is a member of the Flaviviridae family of ≈9.6 kb, and it has a central ORF flanked by the 5′ and 3′ noncoding regions. The ORF is divided into the coding sequences for the structural proteins at the 5′ end and the nonstructural proteins at the 3′ end. Study of the biology of hepatitis C at a molecular level focused initially on expression and manipulation of individual viral proteins in tissue culture.

The development of the subgenomic and genomic replicons is a major breakthrough to understanding viral replication and viral-cell interactions and provides a means to test therapeutic targets (2, 3). However, as yet, none of these systems produce viral particles, nor do they produce infectious virions. Although some infectious tissue culture systems have been described; in general, these systems have not been robust enough to study the complete viral life cycle (4, 5).

Why virion production has been such an elusive goal remains unclear; however, the promise of a system that produces authentic virions is clear. Not only would more of the biology of the virus become accessible for study, but also such a system would provide a means to screen a wider range of potential therapeutic compounds. There is evidence for an inverse relationship between viral replication in tissue culture and virulence in the host organism. This relationship is true for hepatitis A, and there is evidence that it may be true for HCV as well (6, 7). Regardless of the reason for this difficulty, there is an urgent need to establish such a system if improved therapies are to be developed, particularly given the absence of a simple small-animal model of HCV infection. This need is especially true for genotype 1, given that this genotype is the major genotype of human infections worldwide and is the type most resistant to current therapies (8, 9).

In this study, we describe an *in vitro* HCV replication system that is capable of producing viral particles in the culture medium. A full-length HCV construct, CG1b of genotype 1b, known to be infectious (10), was placed between two ribozymes designed to generate the exact 5′ and 3′ ends of HCV when cleaved. By using this system, we showed that HCV proteins and positive and negative RNA strands were produced intracellularly, and viral particles that resemble authentic HCV virions were produced and secreted into the culture medium. This system provides a unique opportunity to further study the life cycle and biology of HCV and to test potential therapeutic targets.

Materials and Methods

Plasmid Construction. The ribozymes were constructed by means of three pairs of overlapping primers that were based on a described ribozyme pair that was functional in hepatocytes (11). The innermost set (5′-CGG TAC CCG GTA CCG TCG CCA GCC CCC GA and 3′-ACG GAT CTA GAT CCG TCA CAT GAT CTG CA) was used to amplify pHCVGFP2. The pHCVGFP2 was derived from an infectious full-length HCV CG1b clone (10) and was constructed by replacing the HCV sequences between nucleotide 709 (*Cla*I) and 8935 (*Bgl*II) by the sequence coding for the GFP. The middle (5′-TCC GTG AGG ACG AAA CGG TAC CCG GT and 3′-CAC GGA CTC ATC AGG ACG GAT CTA GA) and outermost (5′-GGC TGG CCT GAT GAG TCC GTG AGG A and 3′-GAT CAT GTT CGT CCT CAC GGA CTC A) sets were then added on to this sequence by PCR. This fragment was cloned into the *Srf*I site of pCMV-Script (Stratagene) and in turn subcloned into pcDNA3.1 (Invitrogen) by using *Not*I and *Hin*dIII sites to generate the pHt plasmid. pcDNA has both a CMV and a T7 promoter. The GFP was then removed, and the missing part of the HCV sequence was reinserted to generate the pHr plasmid. The pHr was used to generate the HCV-ribozyme RNA by T7 polymerase to assess the efficiency of the ribozymes. The HCV-ribozyme fragment was subcloned into pTRE2hyg+ (Clontech) under the control of a tetracycline-responsive promoter. This construct was named pTHr. In all the experiments described in this study, pTHr transfection always refers to cotransfection with pTet-Off (Clontech) expressing the tetracycline-responsive transactivator. A mutation in the GDD motif of the polymerase (GDD→GND)

This work was presented in part at the 55th Annual Meeting of the American Association for the Study of Liver Disease, Boston, October 30–November 2, 2004.

Abbreviation: HCV, hepatitis C virus.

†T.H. and S.S. contributed equally to this work.

§To whom correspondence should be addressed at: Liver Diseases Branch, National Institute of Diabetes and Digestive and Kidney Diseases, National Institutes of Health, Building 10, Room 9B16, 10 Center Drive MSC 1800, Bethesda, MD 20892-1800. E-mail: jliang@nih.gov.

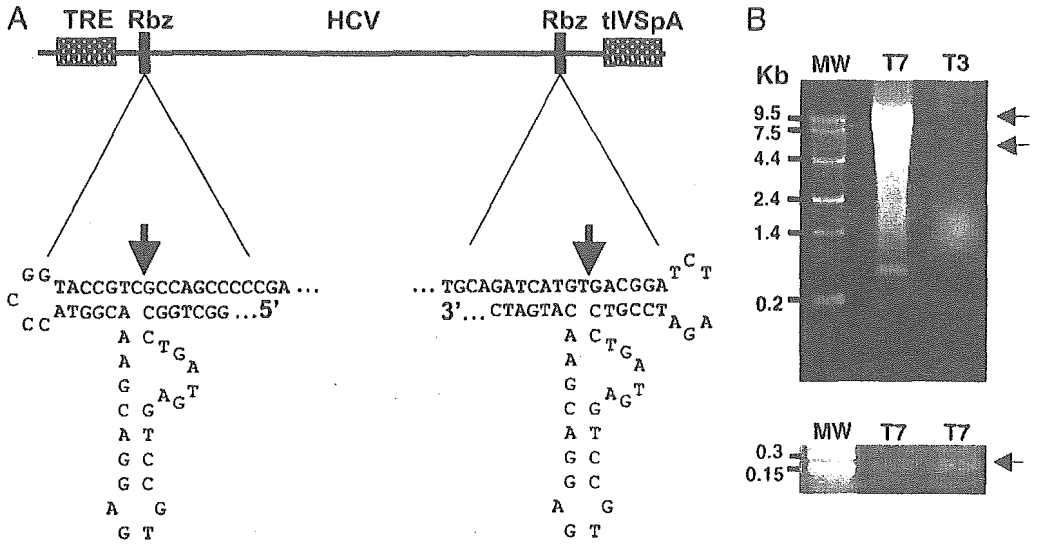

Fig. 1. Construction of HCV-ribozyme plasmid. (*A*) The design of the construct is shown with the positions and sequences of the ribozymes (Rbz) flanking the 5′ and 3′ ends of the HCV CG1B sequence. The cleavage sites are indicated by arrows. The boxes shown 5′ and 3′ to the construct represent the promoter sequence (5′ end) and the simian virus 40 small T antigen intron and polyadenylation signal (3′ end). (*B*) An RNA gel with *in vitro* transcription products from pHr. The first lane shows molecular weight (MW) markers, and the second lane shows a sense transcript beginning at the 5′ end under the control of the T7 promoter. (*Upper*) The expected fragments at ≈9,500 and 5,400 nucleotides are indicated by arrows. The third lane shows an antisense transcript from the 3′ end under the control of a T3 promoter showing bands representing the full length of the plasmid and a population of RNA ≈1,400 bp long that possibly represents a termination sequence or difficult secondary structure at that region. (*Lower*) The expected 150-nt fragment can be seen on this gel with longer exposure (both lanes labeled T7).

was introduced into this construct, and the mutated construct was named pTHrGND. The plasmid pTREhyg2+, without any insert, was also used as a control and is hereon referred to as pTRE.

Tissue Culture and Transfection and RNase Protection Assay. A human hepatoma cell line (Huh7) was maintained at 37°C in Dulbecco's modified Eagle's medium containing 10% FBS with 5% CO_2. Transfection was carried out by using Lipofectamine (Invitrogen) according to the manufacturer's instructions. RPA 111 ribonuclease protection assay kits (Ambion) were used according to the manufacturer's directions. The probe used was transcribed from a construct containing the core region from nucleotide 342 to nucleotide 707 of HCV CG1b strain flanked by the T3 and T7 promoters.

Immunofluorescence and Western Blot. Huh7 cells were grown on glass coverslips and transfected as described. Cells were fixed with acetone/methanol on ice at different time points after transfection. Cells were washed with PBS three times, incubated with primary antibody for 1 h, washed with PBS, incubated with secondary antibody, and washed again with PBS. Monoclonal antibodies against the core (C1) and E1 (A4) were from H. Greenberg (Stanford Medical School, Palo Alto, CA) (12). The anti-E2 monoclonal antibodies AP33 and ALP98 were from A. Patel (Medical Research Council, Glasgow, Scotland) (13). The NS5A monoclonal antibody was obtained from J. Lau (ICN). The Cy3-labeled donkey anti-mouse IgG was obtained from Kirkegaard & Perry Laboratories. The same primary antibodies were used for Western blotting. The peroxidase-labeled goat anti-mouse IgG used as the secondary antibody was obtained from Kirkegaard & Perry Laboratories.

Sucrose Gradient Density Centrifugation. The tissue culture medium was centrifuged to remove cellular debris, and the supernatant was pelleted over a 30% sucrose cushion. The pellet was resuspended in TNC buffer (10 mM Tris·HCl, pH 7.4/1 mM $CaCl_2$/150 mM NaCl) with EDTA-free protease inhibitors (Roche Applied Science) and applied onto a 20–60% sucrose gradient (10.5-ml volume) in SW41 tubes (Beckman Coulter) and centrifuged at 100,000 × *g* for 16 h at 4°C. We collected 1-ml fractions from the top of the gradient. The fractions were tested for HCV proteins and viral RNA as described below. Cryoelectron microscopy was performed by using standard techniques.

HCV RNA, Protein Quantitation, and RACE. HCV RNA level was quantitated by using the TaqMan real-time PCR method as described in ref. 10. RNA was extracted from 100 μl of the sucrose gradient fractions or tissue culture media by using TRIzol (Invitrogen) and resuspended in 20 μl of double-filtered RNase-free water. Samples were tested in duplicate. The core protein was quantitated by using the HCV core ELISA kits, which were provided by S. Yagi (Advanced Life Technology, Saitama, Japan) and used as described in ref. 14. Samples were tested in 50- or 100-μl aliquots. RNA was extracted by using TRIzol (Invitrogen), reverse-transcribed, and amplified by RNA ligase-mediated RACE (RLM-RACE, Ambion). The 5′ and 3′ RACE procedure was performed as described in ref. 15.

Results

Ribozyme Activity. To prove that the ribozymes function properly in the context of HCV genome, the HCV-ribozyme RNA was generated by *in vitro* transcription of pHr and analyzed by formamide gel electrophoresis. The results are shown in Fig. 1*B*. A band corresponding to the full-length HCV genome of ≈9,587 nt was detected. Also seen were bands corresponding to the vector (5,400 nt), a 150-nt fragment corresponding to the RNA between the T7 transcription initiation and the cleavage site of the 5′ ribozyme, and other molecular weight fragments probably representing uncleaved or prematurely terminated transcripts. A similarly expected pattern of cleavage was also observed with the pHt, which is the precursor construct of the pHr and contains the GFP sequence in place of the HCV polyprotein sequence (data not shown). Further proof of the ribozymes cleaving correctly is discussed later with the RACE results.

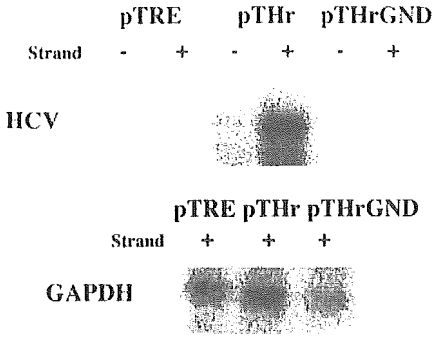

Fig. 2. Detection of HCV positive- and negative-strand RNAs. (*Upper*) The experiment. Shown are the total cellular RNA probed for the HCV core sequence, either positive or negative strand, and the findings when cellular RNA from pTRE-, pTHr-, or pTHrGND-transfected cells were probed for either positive- or negative-strand core sequence. (*Lower*) The control. Shown is the total cellular RNA probed for GAPDH messenger RNA. Note that the amounts are roughly comparable in the three lanes.

HCV RNA and Protein Production in Transfected Cells. Both positive- and negative-strand HCV RNAs were detected in cells transfected with pTHr (Fig. 2). The level of positive-strand HCV RNA was at least 10-fold higher than the level of negative-strand HCV RNA in multiple experiments. The GND mutant pTHrGND produced a small amount of positive-strand RNA but did not produce any detectable negative-strand RNA. The positive-strand RNA produced with the GND mutant was less than that produced with pTHr. No viral RNA was detected in cell lysates transfected with pTRE.

Cells transfected with pTHr or the control plasmid pTRE were analyzed by immunofluorescence with monoclonal antibodies directed against the core, E2, and NS5A. A granular cytoplasmic staining was seen with antibodies against all three proteins (Fig. 3). A time-course experiment showed peak protein expression on day 2 and a significant decrease on day 4 after transfection (data not shown). The percentage of cells with fluorescence was ≈10%, despite the transfection efficiency of ≈50% with a GFP-containing plasmid (data not shown). No immunofluorescence was seen in the cells transfected with pTRE.

Western blot of cell lysates transfected with pTRE or pTHr showed the presence of core, E2, and NS5A in cells transfected with pTHr but not in cells transfected with pTRE (Fig. 4). As expected, viral protein was not detected in the presence of doxycycline (data not shown). Furthermore, little or no HCV protein was detected in pTHrGND-transfected cells, suggesting that viral replication is required for efficient protein production in this system (data not shown).

HCV Virion Production and Secretion. To assess the possibility of HCV particle production, culture medium of the pTHr- and pTHrGND-transfected cells was subjected to sucrose density gradient centrifugation. The fractions were analyzed for two HCV structural proteins, core and E2, and HCV RNA. These results are shown in Fig. 5*A*. In the culture medium from cells transfected with pTHr, a peak of HCV proteins and RNA coincided in fraction 5, which has the density of 1.16 g/ml. This density is consistent with the published density of free HCV virions (16). Viral particles were visualized by electron microscopy only in fraction 5 (Fig. 5*B*). These particles are heterogeneous in appearance and have at least two sizes (≈50 and 100 nm in diameter) with the 50 nm being the major form. This heterogeneity has been described in ref. 17. Viral particles are double-shelled and appear to have spike-like projections from their surface. Shown in Fig. 5*A* are the results for pTHrGND-transfected cells. The HCV protein and RNA levels are at least 10-fold less than those of the pTHr-transfected cells.

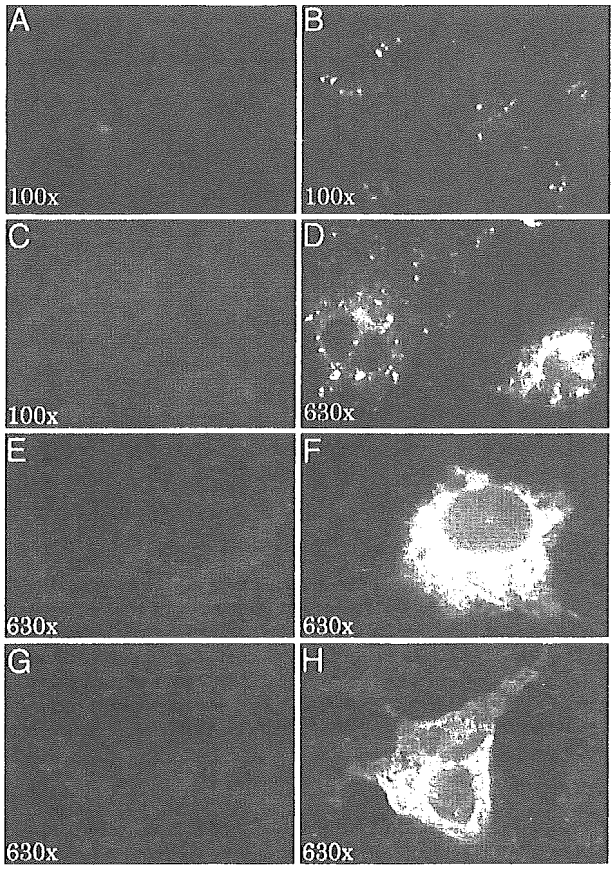

Fig. 3. Detection of HCV proteins by immunofluorescence. (*A*) Low-power view of cells transfected with pTHr and stained without primary antibody but with the secondary antibody. No fluorescence was seen. (*B*) Low-power view of cells transfected with pTHr and stained with anti-core. Multiple cells with fluorescence can be seen. (*C*) Low-power view of cells transfected with the control pTRE and stained with anti-core. There was no fluorescence. (*D*) High-power view of *B*. (*E* and *F*) High-power views of cells stained with anti-E2. Cells were transfected with pTRE (*E*) or pTHr (*F*). (*G* and *H*) High-power views of cells transfected with pTRE (*G*) and pTHr (*H*) and stained with anti-NS5A .

RACE. RACE was used to ensure the exact cleavage of the 5′ and 3′ ends of HCV by the ribozymes. *In vitro*-transcribed RNA from pHr and RNA from the culture medium of pTHr-transfected cells were analyzed by RACE. The 5′ end of the *in vitro*-transcribed RNA, as expected, had the same sequence as the cDNA construct (Fig. 6*A*). However the 3′ end of the *in vitro* transcript could not be amplified by RACE, possibly because of a less efficient cleavage by the 3′ ribozyme and subsequent difficulty in amplifying a heterogeneous population of the 3′ ends. Both the 5′ and 3′ ends of HCV RNA from the culture medium were successfully determined. Interestingly, a change in

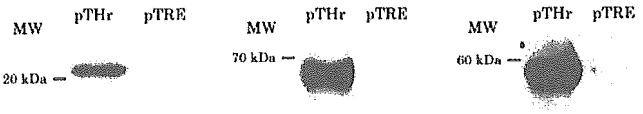

Fig. 4. Detection of HCV proteins by Western blot. In each blot, the first lane shows cells transfected with pTHr and the second lane shows cells transfected with pTRE. The molecular weights are shown on the left of the blots. (*Left*) Blot was probed with anti-core. (*Center*) Blot probed with anti-E2. (*Right*) Blot probed with anti-NS5A.

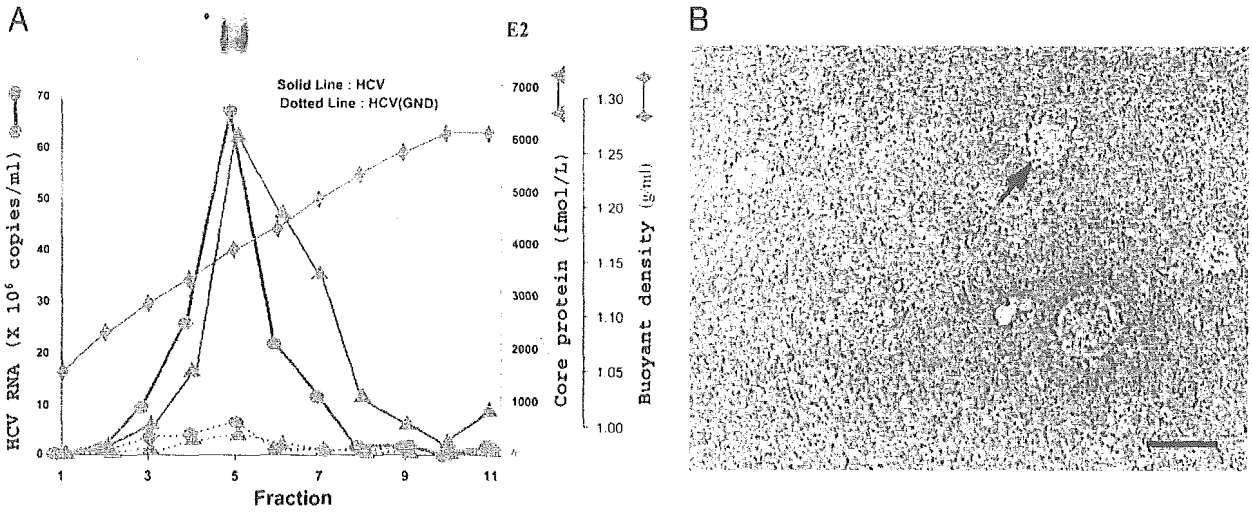

Fig. 5. Sucrose density gradient analysis of culture medium of HCV-transfected cells. (*A*) (*Lower*) Results of the sucrose gradient for pTHr (solid lines) and pTHrGND (dotted lines) transfections. The buoyant density of the sucrose is plotted with the levels of HCV RNA measured by TaqMan PCR and HCV core protein measured by core ELISA. (*Upper*) Western blot for the E2 protein in the fractions of the sucrose gradient of the pTHr transfection. Each lane corresponds to the fraction number below it on the *x* axis of the graph. Three hundred microliters of each fraction was spun at 100,000 × *g* for 90 min, and the pellet was resuspended in loading buffer and used for the Western blot. (*B*) Cryoelectron microscopy of fraction 5. (Bar, 100 nm.)

the most 5′ nucleotide from G to A was noted; this change has been frequently observed in HCV RNA replicons and circulating HCV RNA in infected humans (15). In the 3′ end, two nucleotide changes in the stem loop region were noted: U→A and A→U. These changes preserved the stem loop structure (Fig. 6*B*). Such changes have also been reported in HCV RNA from infected individuals (18). The RNA levels in the medium of the GND-transfected cells were not adequate to perform RACE.

Discussion

Since the discovery of HCV in 1989, working with HCV has proven to be difficult, mostly because of the lack of model systems (19). Each aspect of the life cycle has been difficult to reproduce *in vitro*. The infectious clone was developed after multiple attempts and had to be demonstrated in a chimpanzee (20, 21). Other small-animal models require complicated systems (22, 23). *In vitro*, virus obtained from infected individuals can replicate only in certain B cell lines and primary human

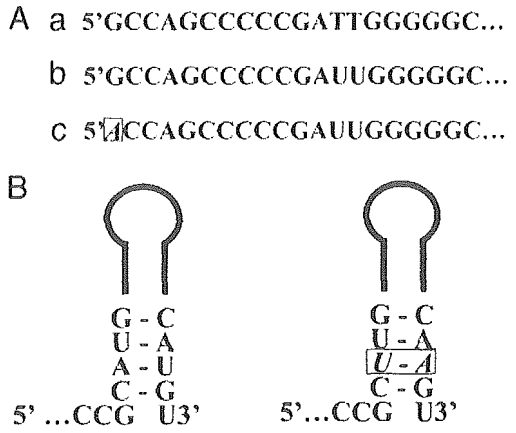

Fig. 6. Sequences of the 5′ and 3′ ends of HCV RNA. (*A*) The cDNA sequence for the 5′ end of the CG1B strain (*a*) and the RACE results for the 5′ ends of *in vitro*-transcribed RNA (*b*) and of the HCV RNA from the culture medium (*c*). (*B*) The cDNA sequences and the stem-loop structures of the 3′ ends of the CG1b strain (*Left*) and the HCV RNA from the medium (*Right*). Nucleotide changes are boxed.

hepatocytes but only at a low level (4, 5). Until the development of the replicon, most model systems have been difficult to work with (2, 24). Development of virus-like particles and pseudovirus have allowed study of viral entry into the cell but do not model other aspects of the viral life cycle (25–28). Therefore, a model system with viral replication, assembly, and release is urgently needed. Furthermore, genotype 1, the most prevalent form of HCV and the most difficult to treat, was chosen for this model.

By engineering two hammerhead ribozyme sequences, one at the 5′ end and the other at the 3′ end of an infectious HCV cDNA clone, we generated a DNA expression construct for the production of HCV virions. An important initial consideration was to ensure that the ribozymes are indeed functional. This functionality was demonstrated by *in vitro*-translation and RACE. Transfection of this HCV-ribozyme construct into Huh7 cells demonstrated the production of structural and nonstructural proteins by immunofluorescence and Western blot. Both positive- and negative-strand RNAs could be detected intracellularly. As expected, the positive strand is much more abundant than the negative strand.

The GND mutant was constructed as a control to determine the extent of replication in this model. Evidence for replication was derived from a number of results. The simplest evidence was the presence of negative-strand viral RNA in pTHr-transfected cells and the lack of negative strand in pTHrGND-transfected cells. A >10-fold difference in the relative amounts of the positive-strand viral RNA between the wild-type and GND constructs provided additional evidence. This observation can be explained by the lack of amplification as a result of defective replication. The positive strand seen with the GND mutant was generated from transcription of the cDNA plasmid. This difference in product was also evident in the culture medium. The amounts of viral RNA and core protein on the sucrose gradients were >10-fold higher in wild-type cells than in the GND mutant-transfected cells. The final and perhaps the most interesting evidence for replication is the RACE findings. The 5′ and 3′ nucleotide changes have been described in refs. 15 and 18. The G→A switch of the initial nucleotide of HCV is associated with replication *in vivo* and *in vitro* (15). A transposition from an A–T to a T–A base pairing has also been reported (18) and represents a base pair in the putative terminal stem loop of the 3′ end of

HCV. These observations provide support for the replication of viral RNA in this system.

Evidence for assembly and release was derived in a number of ways. The presence of HCV RNA in the media with the exact 5′ and 3′ ends showed that the correctly processed RNA was secreted into the culture medium. The association of viral RNA and core and E2 protein in the same fraction on the sucrose gradient with a density of 1.16g/ml (the published density of free HCV virions) supported the interpretation that viral particles are assembled and secreted into the medium. The most compelling evidence is the visualization of particles resembling virions by electron microscopy, and these particles were visualized only in fraction 5, where viral RNA and proteins are present. It is interesting that the core protein extends into fractions 6 and 7 more than the viral RNA and E2 protein. This core reactivity might represent free core particles, although they were not seen on electron microscopy (29). The production and release of HCV particles is rather robust in this system, capable of achieving >10 million copies of HCV RNA per ml in the culture medium.

Although replicons using the full-length HCV genome have been developed, particles have not been described. In those replicons where sequence coding for the neomycin is included, difficulty in packaging a longer RNA molecule might be the problem. Alternatively the block could be the result of the inhibitory effects of the replicon adaptive mutations on virion assembly and release. Both possibilities are speculative. However, in the system presented here, there is no extraneous RNA and, although mutations can and do occur (see the RACE results), the source of the RNA (the cDNA) maintains a stable sequence without adaptive mutations. This difference might partially explain why particles are seen. It may also be of importance that there is a constant RNA production inside the cells being channeled directly into the appropriate cellular machinery for assembly.

This model system does not allow the study of viral entry and the earliest events in the HCV life cycle. In addition, whether these particles are infectious or not remains to be determined. The HCV sequence used is known to be infectious in chimpanzees. It should be noted that the sequence is genotype 1b. The results that would be obtained with other genotypes in this system is unknown. Despite these caveats, it represents a robust system to study the viral life cycle, specifically viral assembly and release. Very little is known about the assembly and release of HCV. This work might present an opportunity to better elucidate the biology of HCV as well as to develop therapeutic targets for the treatment of hepatitis C, in particular for genotype 1.

Note Added in Proof. During the preparation of this manuscript, two groups (T. Wakita, T. Takanobu, T. Date, and M. Miyamoto and T. Pietschmann, G. Koutsoudakis, S. Kallis, T. Kato, S. Foung, T. Wakita, and R. Bartenschlager) at the 11th International Symposium on HCV and Related Viruses (Heidelberg, Germany, Oct. 3–7, 2004) reported the production of infectious HCV in cell culture by transfecting a full-length HCV RNA genome.

We thank Z. Hong Zhou, Ph.D., for superb cryoelectron microscopy, Shintaro Yagi for providing the HCV core ELISA kit, and Anthony Davis for excellent technical assistance.

1. Liang, T. J., Rehermann, B., Seeff, L. B. & Hoofnagle, J. H. (2000) *Ann. Intern. Med.* **132,** 296–305.
2. Lohmann, V., Korner, F., Koch, J., Herian, U., Theilmann, L. & Bartenschlager, R. (1999) *Science* **285,** 110–113.
3. Ikeda, M., Yi, M., Li, K. & Lemon, S. M. (2002) *J. Virol.* **76,** 2997–3006.
4. Shimizu, Y. K., Iwamoto, A., Hijikata, M., Purcell, R. H. & Yoshikura, H. (1992) *Proc. Natl. Acad. Sci. USA* **89,** 5477–5481.
5. Sung, V. M., Shimodaira, S., Doughty, A. L., Picchio, G. R., Can, H., Yen, T. S., Lindsay, K. L., Levine, A. M. & Lai, M. M. (2003) *J. Virol.* **77,** 2134–2146.
6. Raychaudhuri, G., Govindarajan, S., Shapiro, M., Purcell, R. H. & Emerson, S. U. (1998) *J. Virol.* **72,** 7467–7475.
7. Bukh, J., Pietschmann, T., Lohmann, V., Krieger, N., Faulk, K., Engle, R. E., Govindarajan, S., Shapiro, M., St Claire, M. & Bartenschlager, R. (2002) *Proc. Natl. Acad. Sci. USA* **99,** 14416–14421.
8. Manns, M. P., McHutchison, J. G., Gordon, S. C., Rustgi, V. K., Shiffman, M., Reindollar, R., Goodman, Z. D., Koury, K., Ling, M. & Albrecht, J. K. (2001) *Lancet* **358,** 958–965.
9. Fried, M. W., Shiffman, M. L., Reddy, K. R., Smith, C., Marinos, G., Goncales, F. L., Jr., Haussinger, D., Diago, M., Carosi, G., Dhumeaux, D., *et al.* (2002) *N. Engl. J. Med.* **347,** 975–982.
10. Thomson, M., Nascimbeni, M., Gonzales, S., Murthy, K. K., Rehermann, B. & Liang, T. J. (2001) *Gastroenterology* **121,** 1226–1233.
11. Benedict, C. M., Pan, W., Loy, S. E. & Clawson, G. A. (1998) *Carcinogenesis* **19,** 1223–1230.
12. Dubuisson, J., Hsu, H. H., Cheung, R. C., Greenberg, H. B., Russell, D. G. & Rice, C. M. (1994) *J. Virol.* **68,** 6147–6160.
13. Triyatni, M., Saunier, B., Maruvada, P., Davis, A. R., Ulianich, L., Heller, T., Patel, A., Kohn, L. D. & Liang, T. J. (2002) *J. Virol.* **76,** 9335–9344.
14. Tanaka, E., Ohue, C., Aoyagi, K., Yamaguchi, K., Yagi, S., Kiyosawa, K. & Alter, H. J. (2000) *Hepatology* **32,** 388–393.
15. Cai, Z., Liang, T. J. & Luo, G. (2004) *J. Virol.* **78,** 3633–3643.
16. Kaito, M., Watanabe, S., Tsukiyama-Kohara, K., Yamaguchi, K., Kobayashi, Y., Konishi, M., Yokoi, M., Ishida, S., Suzuki, S. & Kohara, M. (1994) *J. Gen. Virol.* **75,** 1755–1760.
17. Andre, P., Komurian-Pradel, F., Deforges, S., Perret, M., Berland, J. L., Sodoyer, M., Pol, S., Brechot, C., Paranhos-Baccala, G. & Lotteau, V. (2002) *J. Virol.* **76,** 6919–6928.
18. Kolykhalov, A. A., Feinstone, S. M. & Rice, C. M. (1996) *J. Virol.* **70,** 3363–3371.
19. Choo, Q. L., Kuo, G., Weiner, A. J., Overby, L. R., Bradley, D. W. & Houghton, M. (1989) *Science* **244,** 359–362.
20. Kolykhalov, A. A., Agapov, E. V., Blight, K. J., Mihalik, K., Feinstone, S. M. & Rice, C. M. (1997) *Science* **277,** 570–574.
21. Yanagi, M., Purcell, R. H., Emerson, S. U. & Bukh, J. (1997) *Proc. Natl. Acad. Sci. USA* **94,** 8738–8743.
22. Mercer, D. F., Schiller, D. E., Elliott, J. F., Douglas, D. N., Hao, C., Rinfret, A., Addison, W. R., Fischer, K. P., Churchill, T. A., Lakey, J. R., *et al.* (2001) *Nat. Med.* **7,** 927–933.
23. Labonte, P., Morin, N., Bowlin, T. & Mounir, S. (2002) *J. Med. Virol.* **66,** 312–319.
24. Blight, K. J., Kolykhalov, A. A. & Rice, C. M. (2000) *Science* **290,** 1972–1974.
25. Baumert, T. F., Ito, S., Wong, D. T. & Liang, T. J. (1998) *J. Virol.* **72,** 3827–3836.
26. Nam, J. H., Bukh, J., Purcell, R. H. & Emerson, S. U. (2001) *J. Virol. Methods* **97,** 113–123.
27. Bartosch, B., Bukh, J., Meunier, J. C., Granier, C., Engle, R. E., Blackwelder, W. C., Emerson, S. U., Cosset, F. L. & Purcell, R. H. (2003) *Proc. Natl. Acad. Sci. USA* **100,** 14199–14204.
28. Logvinoff, C., Major, M. E., Oldach, D., Heyward, S., Talal, A., Balfe, P., Feinstone, S. M., Alter, H., Rice, C. M. & McKeating, J. A. (2004) *Proc. Natl. Acad. Sci. USA* **101,** 10149–10154.
29. Maillard, P., Krawczynski, K., Nitkiewicz, J., Bronnert, C., Sidorkiewicz, M., Gounon, P., Dubuisson, J., Faure, G., Crainic, R. & Budkowska, A. (2001) *J. Virol.* **75,** 8240–8250.